KINEMATICS MODELLING OF A SPATIAL TWO-MODULE HYBRID PARALLEL ROBOT

Stefan STAICU [1]

Matrix relations for kinematics analysis of a spatial two-module hybrid parallel mechanism are established in this paper. Knowing the relative motions of the moving platforms, the inverse kinematics problem is solved based on a set of connectivity relations. Finally, compact results and graphs of simulation for the input relative displacements, velocities and accelerations are obtained.

Keywords: Connectivity relations; Hybrid parallel robot; Kinematics

1 Introduction

Provided with closed-loop structures, the links of parallel robots can be connected one to the other by spherical joints, universal joints, revolute joints or prismatic joints. Compared with traditional serial manipulators, the compactness, accuracy and precision in the direction of the tasks are essential for the parallel architectures [1], [2].

During last three decades, considerable efforts have been devoted to the kinematics and dynamics of parallel robots. Among these, the class of manipulators known as Stewart-Gough platform, used in flight simulators, focused great attention (Di Gregorio and Parenti Castelli [3]). The prototype of Delta parallel robot (Clavel [4]; Tsai and Stamper [5]) and the Star parallel manipulator (Hervé and Sparacino [6]) are equipped with three motors, which train on the mobile platform in a general translation motion. Angeles [7], Wang and Gosselin [8] analysed the kinematics, singularity loci and determined the workspace of spherical Agile Wrist robot with three concurrent actuators.

A hybrid manipulator is a combination of closed-chain and open-chain mechanisms or a sequence of parallel robots [9], [10], [11]. A serial-parallel manipulator has several modules with parallel structure that are connected serially. This kind of hybrid architectures posses the advantages of both serial and parallel manipulators from rigidity, accuracy and workspace point of view.

Shahinpoor [12] obtained and solved numerically a system of nonlinear equations for the inverse kinematics problem of a hybrid robotic system

[1] Professor Emeritus, Department of Mechanics, University POLITEHNICA of Bucharest, ROMANIA

consisting of two serially connected parallel manipulators. Cheng et al. [13] used a numerical Newton-Raphson method to obtain the solution of the direct kinematics problem of a 10-DOF hybrid redundant manipulator, containing a closed-loop slider-crank mechanism and a parallel-driven mechanism. Considering the lower module as a positional mechanism and the upper as an orientation device, Zhang and Song [14] analyzed the geometry and the position of a hybrid manipulator composed of two serially connected parallel robots, each mechanism having three degrees of freedom. Based on screw theory and principle of virtual work, Gallardo et al. [15] addressed a complete kinematics analysis of a modular spatial hyper-redundant manipulator built with a variable number of serially connected mechanical modules.

A recursive method based on connectivity relations is applied in the present paper to the analysis of a spatial two-module hybrid manipulator, reducing together the number of equations and computation operations significantly by using a set of matrices for kinematics model.

2 Kinematics analysis

The hybrid robot here analyzed is made up of two 3-DOF similar parallel modules, which are serially connected to a fixed base, but the study can be easily extended to a complex robotic system composed of a multitude serially connected parallel robots. The structure of lower parallel module, for example, consists of a fixed base, a circular mobile platform and four kinematical chains, including three variable length legs with identical topology and one passive constraining leg; the overall degrees of freedom for the hybrid robot are six (Fig. 1).

The two moving platforms are initially considered at a *central configuration*, where are not rotated with respect to the fixed frame and their centers are located at given elevations above the origin O of fixed base. For the purpose of analysis, we assign a fixed Cartesian coordinate system $Ox_0y_0z_0$ at the point O of the fixed frame and also two appropriate mobile frames $G_4x_4^Gy_4^Gz_4^G$ and $H_4x_4^Hy_4^Hz_4^H$ on the moving platforms at their mass centers $G_3 = G_4$ and $H_3 = H_4$, respectively. The first legs $A\,(\alpha_A = 0)$ and D $(\alpha_D = 0)$ of lower and upper modules are initially contained within the Ox_0z_0 vertical plane, whereas the planes of legs B, C and E, F make the angles $\alpha_B = \alpha_E = 120^0$ and $\alpha_C = \alpha_F = -120^0$ with Ox_0z_0 (Fig. 2).

The active leg A of lower module, for example, consists of a little cross of a fixed universal joint linked at the frame $A_1x_1^Ay_1^Az_1^A$ which has the angular velocity $\omega_{10}^A = \dot{\varphi}_{10}^A$ and the angular acceleration $\varepsilon_{10}^A = \dot{\omega}_{10}^A$, connected at a moving cylinder $A_2x_2^Ay_2^Az_2^A$ of length l_2, having a relative rotation around $A_2z_2^A$ axis with the angle φ_{21}^A, so that $\omega_{21}^A = \dot{\varphi}_{21}^A$, $\varepsilon_{21}^A = \dot{\omega}_{21}^A$. An actuated prismatic joint is as well as a piston of length l_3, linked to the $A_3x_3^Ay_3^Az_3^A$ frame, having a relative velocity $v_{32}^A = \dot{\lambda}_{32}^A$ and acceleration $\gamma_{32}^A = \dot{v}_{32}^A$. Finally, a ball-joint A_4 is introduced at the edge of lower moving platform. The fourth constraining chain has a different architecture. It consists of a prismatic joint attached to the fixed base and a moving link of length l_1, having a known purely relative vertical displacement λ_{10}^G, velocity $v_{10}^G = \dot{\lambda}_{10}^G$ and acceleration $\gamma_{10}^G = \dot{v}_{10}^G$.

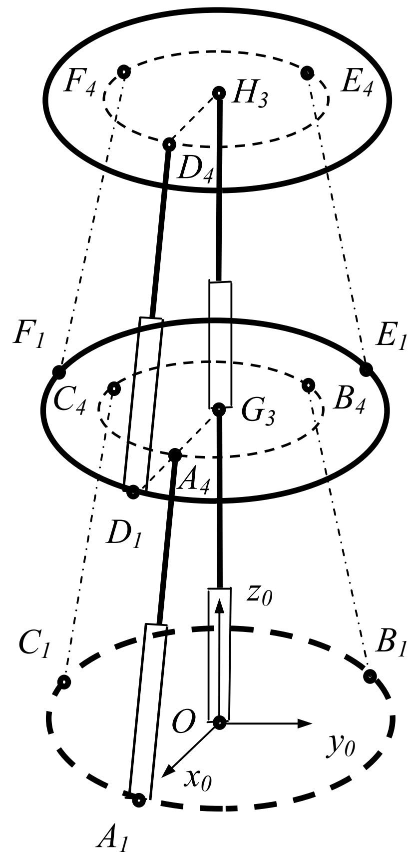

Fig. 1 Symmetric spatial hybrid parallel robot

A little cross of a new universal joint is attached to the center of the first moving platform which can be schematised as a circle of radius r_p. Two successive concurrent rotations of this platform are defined in the local coordinates $G_2x_2^Gy_2^Gz_2^G$ and $G_3x_3^Gy_3^Gz_3^G$ by given angles φ_{21}^G and φ_{32}^G.

At the central configuration, we also consider that six active sliders and two passive central sliders are initially starting from following relative positions $A_2A_3 = B_2B_3 = ... = F_2F_3 = l_{.5}$, $OG_1 = G_3H_1 = l_6$ and that the orientation angles of the legs are given by

$$\alpha_A = \alpha_D = 0, \alpha_B = \alpha_E = \frac{2\pi}{3}, \alpha_C = \alpha_F = -\frac{2\pi}{3}$$

$$(l_3 + l_5)\cos\beta = l_0 - l_4,\ (l_3 + l_5)\sin\beta = l_1 + l_6, \tag{1}$$

where β is an angle of initial inclination.

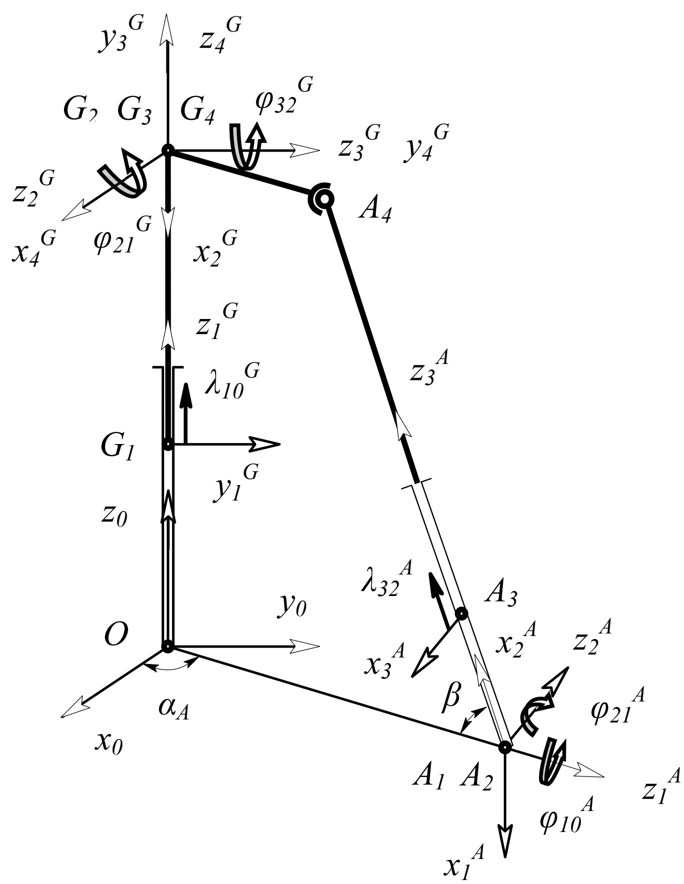

Fig. 2 Kinematical scheme of first leg A of lower module

Since the hybrid manipulator is an assemblage of links and joints, this can be symbolised in a more abstract form known as equivalent graph representation, using the associated graph to represent the topology of the mechanism (Fig. 3). In the kinematical graph representation, with *six independent loops*, the links are denoted by vertices, the prismatic joints by thick edges, the revolute and spherical joints by thin edges and, finally, the fixed link 0 by two small concentric circles.

Considering the passive constraining legs along the *principal kinematical chain* $OG_1G_2G_3G_4H_1H_2H_3H_4$, which connect the moving platforms, relative matrices of transformation are derived [16]

$$p_{10} = I,\, p_{21} = p_{21}^{\varphi}\theta_1,\, p_{32} = p_{32}^{\varphi}\theta_1\theta_2,\, p_{43} = \theta_2\theta_1\theta_2$$
$$p_{20} = p_{21}p_{10},\, p_{30} = p_{32}p_{20},\, p_{40} = p_{43}p_{30} \quad (p = g, h), \tag{2}$$

where the angles $\varphi_{21}^i, \varphi_{32}^i, (i = G, H)$ characterise the sequence of concurrent rotations around the universal joints G_2 and H_2 through following matrices

$$p_{\sigma,\sigma-1}^{\varphi} = rot(z, \varphi_{\sigma,\sigma-1}^i) \;\; (\sigma = 2, 3). \tag{3}$$

Now, starting successively from two reference origins O, G_4 and pursuing six independent legs $OA_1A_2A_3$, $OB_1B_2B_3$, $OC_1C_2C_3$, $G_4D_1D_2D_3$, $G_4E_1E_2E_3$, $G_4F_1F_2F_3$, we obtain new transformation matrices

$$q_{10} = q_{10}^{\varphi}\theta_1 a_{\alpha}^j,\, q_{21} = q_{21}^{\varphi}a_{\beta}\theta_1\theta_2,\, q_{32} = \theta_1,\, q_{20} = q_{21}q_{10},\, q_{30} = q_{32}q_{20} \tag{4}$$

$$(q = a, b, c, d, e, f) \;\; (j = A, B, C, D, E, F),$$

where we denote the matrices

$$q_{\tau,\tau-1}^{\varphi} = rot(z, \varphi_{\tau,\tau-1}^j) \quad (\tau = 1, 2) \tag{5}$$

$$a_{\alpha}^j = rot(z, \alpha_j),\, a_{\beta} = rot(z, \beta),\, \theta_1 = rot(y, \pi/2),\, \theta_2 = rot(z, \pi/2).$$

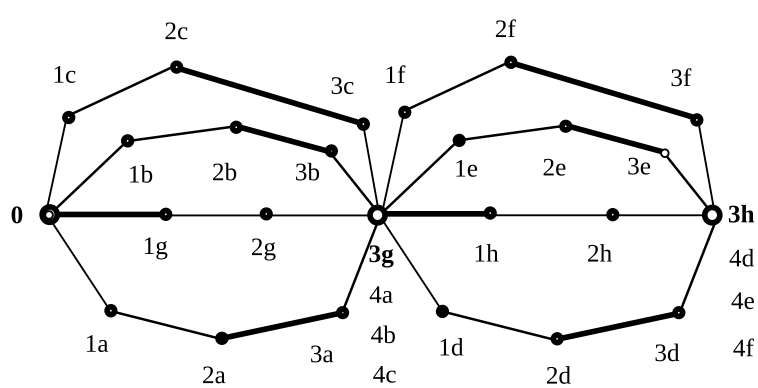

Fig. 3 Associated graph of the mechanism

In a forward geometric problem, the orientation and the position of the serial-parallel robotic system is completely given through the angles of rotation $\varphi_{\sigma,\sigma-1}^i$ and the relative coordinates $z_0^i = l_1 + l_6 + \lambda_{10}^i$ of mass centers of two mobile platforms.

Consider, for example, that during three seconds the coordinates of the centers and the orientation angles can describe the relative motions of the platforms through the following analytical functions

$$\frac{\lambda_{10}^{i}}{\lambda_{10}^{i*}} = \frac{\varphi_{\sigma,\sigma-1}^{i}}{\varphi_{\sigma,\sigma-1}^{i*}} = 1 - \cos\frac{\pi}{3}t \quad (\sigma = 2, 3) \quad (i = G, H)\,. \tag{6}$$

A set of 18 independent variables $\varphi_{\tau,\tau-1}^{j}, \lambda_{32}^{j}$ characterising the kinematics of two modules, will be determined by some vector-loop equations

$$\vec{r}_{10}^{\,j} + \sum_{k=1}^{3} q_{k0}^{T} \vec{r}_{k+1,k}^{\,j} = z_0^i \vec{u}_3 + p_{40}^{T} \vec{r}_i^{\,j_4}\,, \quad 7)$$

where

$$\vec{r}_{10}^{\,j} = l_0 a_\alpha^{jT} \vec{u}_1, \vec{r}_{21}^{\,j} = \vec{0}, \vec{r}_{32}^{\,j} = (l_5 + \lambda_{32}^{j})\vec{u}_1, \vec{r}_{43}^{\,j} = l_3 \vec{u}_3, \vec{r}_i^{\,j_4} = l_4 a_\alpha^{jT} \vec{u}_1 \tag{8}$$

$$\vec{u}_1 = [1\ \ 0\ \ 0]^T,\ \vec{u}_2 = [0\ \ 1\ \ 0]^T,\ \vec{u}_3 = [0\ \ 0\ \ 1]^T$$

$$(p = g, h)\ \ (i = G, H)\ \ (q = a, b, c, d, e, f)\ \ (j = A, B, C, D, E, F)\,.$$

The motion of the compounding elements of the hybrid manipulator are characterized by following relative velocities of joints and angular velocities

$$\vec{v}_{10}^{\,i} = \dot{\lambda}_{10}^{i} \vec{u}_3, \vec{v}_{\sigma,\sigma-1}^{\,i} = \vec{0}, v_{43}^{i} = 0, \vec{v}_{\tau,\tau-1}^{\,j} = \vec{0}, \vec{v}_{32}^{\,j} = \dot{\lambda}_{32}^{j} \vec{u}_3$$

$$\vec{\omega}_{10}^{i} = \vec{0}, \vec{\omega}_{\sigma,\sigma-1}^{i} = \omega_{\sigma,\sigma-1}^{i} \vec{u}_3, \omega_{43}^{i} = 0, \vec{\omega}_{\tau,\tau-1}^{j} = \omega_{\tau,\tau-1}^{j} \vec{u}_3, \vec{\omega}_{32}^{j} = \vec{0} \tag{9}$$

$$(\sigma = 2, 3)\ \ (\tau = 1, 2)\,.$$

To describe the absolute kinematical state of each link of leg j, for example, we compute the linear velocity $\vec{v}_{k0}^{\,j}$, the angular velocity $\vec{\omega}_{k0}^{j}$ and the *associate skew-symmetric matrix* $\tilde{\omega}_{k0}^{j}$ in terms of the vectors of the preceding body, using a recursive manner:

$$\vec{v}_{k0}^{\,j} = q_{k,k-1} \vec{v}_{k-1,0}^{\,j} + q_{k,k-1} \tilde{\omega}_{k-1,0}^{j} \vec{r}_{k,k-1}^{\,j} + v_{k,k-1}^{j} \vec{u}_3$$

$$\vec{\omega}_{k0}^{j} = q_{k,k-1} \vec{\omega}_{k-1,0}^{j} + \omega_{k,k-1}^{j} \vec{u}_3\,,\ \tilde{\omega}_{k0}^{j} = q_{k,k-1} \tilde{\omega}_{k-1,0}^{j} q_{k,k-1}^{T} + \omega_{k,k-1}^{j} \tilde{u}_3\,. \tag{10}$$

Starting from the derivatives of geometrical constraints (7) and using the skew-symmetric matrices

$$\tilde{\omega}_{40}^{i} = \dot{\varphi}_{21}^{i} p_{43} p_{32} \tilde{u}_3 p_{32}^{T} p_{43}^{T} + \dot{\varphi}_{32}^{i} p_{43} \tilde{u}_3 p_{43}^{T} \quad (i = G, H)\,, \tag{11}$$

which are associated to the angular velocities $\vec{\omega}_{40}^{i}$ of two moving platforms, we obtain the *matrix conditions of connectivity* [17], and the relative velocities $\vec{V}_j = [\omega_{10}^{j}\ \ \omega_{21}^{j}\ \ v_{32}^{j}]^T$:

$$\vec{V}_j = [N_j]^{-1}\vec{P}_j \,, \tag{12}$$

where following terms determines the contents of 3x3 invertible square matrix $[N_j]$ and the column matrix $\vec{P}_j$:

$$n_{l1}^j = u_l^T q_{10}^T \tilde{u}_3 q_{21}^T \{\vec{r}_{32}^{\,j} + q_{32}^T \vec{r}_{43}^{\,j}\}\,,\; n_{l2}^j = \vec{u}_l^T q_{20}^T \tilde{u}_3 \{\vec{r}_{32}^{\,j} + q_{32}^T \vec{r}_{43}^{\,j}\}$$

$$n_{l3}^j = \vec{u}_l^T q_{20}^T \vec{u}_1 \,,\; \vec{P}_j = v_{10}^i \vec{u}_l^T \vec{u}_3 + \vec{u}_l^T p_{40}^T \tilde{\omega}_{40}^i \vec{r}_i^{\,j_4}$$

$$(p = g, h)\;\; (i = G, H)\;\; (q = a, b, c, d, e, f)\;\; (j = A, B, C, D, E, F)\;\; (l = 1, 2, 3)\,. \tag{13}$$

From these equations, we obtain the *complete* Jacobian matrix of the hybrid manipulator. This matrix is a fundamental element for the analysis of the robot workspace and the particular configurations of singularities where the spatial robot becomes uncontrollable.

Based on another conditions of connectivity, expressions of relative accelerations $\vec{\Gamma}_j = [\varepsilon_{10}^j \;\; \varepsilon_{21}^j \;\; \gamma_{32}^j]^T$ are obtained from the column matrix [18]

$$\vec{\Gamma}_j = [N_j]^{-1}\vec{S}_j \tag{14}$$

where following terms determine the contents of column matrices $\vec{S}_j = \dot{\vec{P}}_j - [\dot{N}_j]\vec{V}_j$:

$$\begin{aligned} s_l^j = {} & \gamma_{10}^i \vec{u}_l^T \vec{u}_3 + \vec{u}_l^T p_{40}^T \{\tilde{\omega}_{40}^i \tilde{\omega}_{40}^i + \tilde{\varepsilon}_{40}^i\}\vec{r}_i^{\,j_4} - \omega_{10}^j \omega_{10}^j \vec{u}_l^T q_{10}^T \tilde{u}_3 \tilde{u}_3 q_{21}^T \{\vec{r}_{32}^{\,j} + q_{32}^T \vec{r}_{43}^{\,j}\} \\ & - \omega_{21}^j \omega_{21}^j \vec{u}_l^T q_{20}^T \tilde{u}_3 \tilde{u}_3 \{\vec{r}_{32}^{\,j} + q_{32}^T \vec{r}_{43}^{\,j}\} - 2\omega_{10}^j \omega_{21}^j \vec{u}_l^T q_{10}^T \tilde{u}_3 q_{21}^T \tilde{u}_3 \{\vec{r}_{32}^{\,j} + q_{32}^T \vec{r}_{43}^{\,j}\} - \\ & - 2\omega_{10}^j v_{32}^j \vec{u}_l^T q_{10}^T \tilde{u}_3 q_{21}^T \vec{u}_1 - 2\omega_{21}^j v_{32}^j \vec{u}_l^T q_{20}^T \tilde{u}_3 \vec{u}_1 \quad (l = 1, 2, 3)\,. \end{aligned} \tag{15}$$

Following relations give the linear accelerations $\vec{\gamma}_{k0}^{\,j}$, the angular accelerations $\vec{\varepsilon}_{k0}^{\,j}$ and the *significant matrices* $\tilde{\omega}_{k0}^j \tilde{\omega}_{k0}^j + \tilde{\varepsilon}_{k0}^j$ of links from the leg j, for example:

$$\begin{aligned} & \vec{\gamma}_{k0}^{\,j} = q_{k,k-1}\vec{\gamma}_{k-1,0}^{\,j} + q_{k,k-1}\{\tilde{\omega}_{k-1,0}^j \tilde{\omega}_{k-1.0}^j + \tilde{\varepsilon}_{k-1,0}^j\}\vec{r}_{k,k-1}^{\,j} + 2v_{k,k-1}^j q_{k,k-1}\tilde{\omega}_{k-1,0}^j q_{k,k-1}^T \vec{u}_3 + \gamma_{k,k-1}^j \vec{u}_3 \\ & \vec{\varepsilon}_{k0}^{\,j} = q_{k,k-1}\vec{\varepsilon}_{k-1,0}^{\,j} + \varepsilon_{k,k-1}^j \vec{u}_3 + \omega_{k,k-1}^j q_{k,k-1}\tilde{\omega}_{k-1,0}^j q_{k,k-1}^T \vec{u}_3 \\ & \tilde{\omega}_{k0}^j \tilde{\omega}_{k0}^j + \tilde{\varepsilon}_{k0}^j = q_{k,k-1}\{\tilde{\omega}_{k-1,0}^j \tilde{\omega}_{k-1,0}^j + \tilde{\varepsilon}_{k-1,0}^j\}q_{k,k-1}^T + \\ & \qquad + \omega_{k,k-1}^j \omega_{k,k-1}^j \tilde{u}_3 \tilde{u}_3 + \varepsilon_{k,k-1}^j \tilde{u}_3 + 2\omega_{k,k-1}^j q_{k,k-1}\tilde{\omega}_{k-1,0}^j q_{k,k-1}^T \tilde{u}_3\,. \end{aligned} \quad 16)$$

As application let us consider a serial-parallel hybrid mechanism which has following kinematical and architectural characteristics

$\varphi_{21}^{G*} = \varphi_{32}^{H*} = \pi/18$, $\varphi_{32}^{G*} = \varphi_{21}^{H*} = \pi/36$, $\lambda_{10}^{G*} = 0.05m$, $\lambda_{10}^{H*} = 0.05m$

$l_1 = 0.65m$, $l_2 = 0.85m$, $l_3 = 0.85m$, $G_3A_4 = H_3D_4 = l_4 = 0.45m$, $l_5 = l_6 = 0.25m$

$\sin\beta = (l_1 + l_6)/(l_3 + l_5)$, $OA_1 = G_3D_1 = l_0 = r_p = (l_3 + l_5)\cos\beta + l_4$.

Assuming that the robot starts at rest from a central configuration, the MATLAB software for a computer program was developed to solve a complete inverse kinematics of the hybrid parallel mechanism.

Two examples are solved to illustrate the algorithm.

For the first example, the platforms move along the *vertical direction* z_0 with variable accelerations while all the other positional parameters are held equal to zero. The time-histories for the input displacements λ_{32}^{j} (Fig. 4), relative velocities v_{32}^{j} (Fig. 5) and relative accelerations γ_{32}^{j} (Fig. 6) are calculated for a period of $\Delta t = 3$ seconds in terms of given analytical equations (6). As can be seen, it is proved to be true that all relative displacements, velocities and accelerations of two modules are permanently equal to one another.

In the second case when the platforms make simultaneously two given *general relative motions*, the graphs are plotted and sketched in Fig. 7, Fig. 8 and Fig. 9

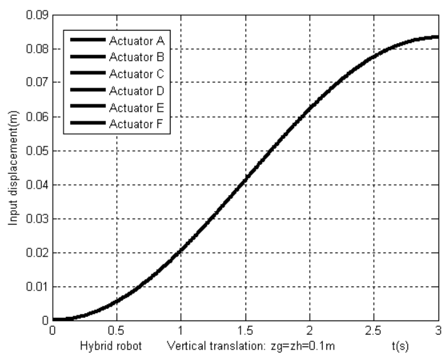

Fig. 4 Input displacements λ_{32}^{j} of six sliders

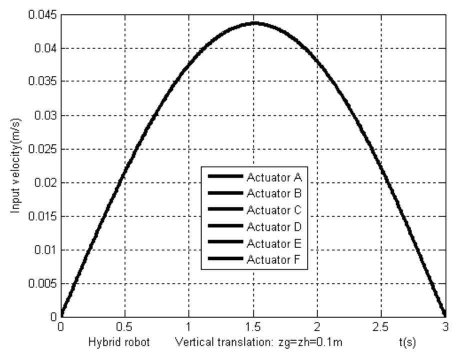

Fig. 5 Input velocities v_{32}^{j} of six sliders

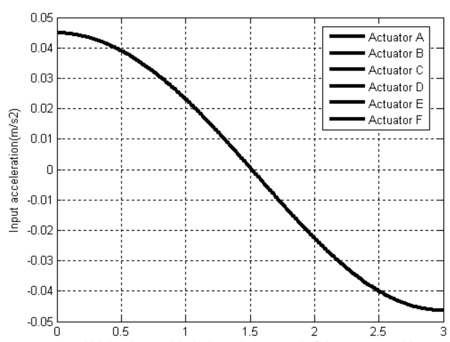

Fig. 6 Input accelerations γ_{32}^{j} of six sliders

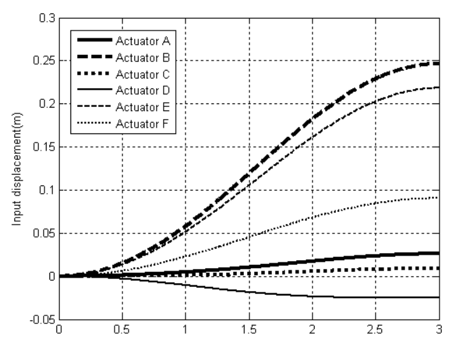

Fig. 7 Input displacements λ_{32}^{j} of six sliders

The simulation through the program certifies that one of the major advantages of the current matrix recursive formulation is accuracy and a smaller processing time of numerical computation.

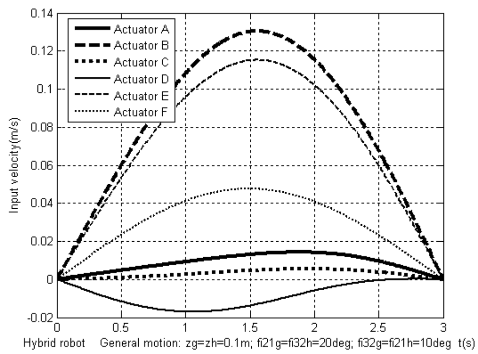

Fig. 8 Input velocities v_{32}^{j} of six sliders

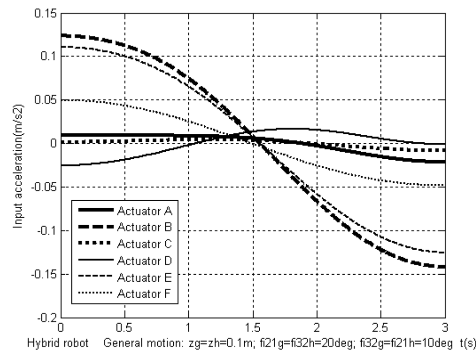

Fig. 9 Input accelerations γ_{32}^{j} of six sliders

3 Conclusions

Some exact relations that give in real-time the position, velocity and acceleration of each element of a two-module hybrid parallel robot have been established in the present paper. Choosing the appropriate serial kinematical circuits connecting many moving platforms, the present concept and the procedure above developed can be immediately extended to analysis of a complex robotic system composed of a multitude serially arranged similar parallel modules, but are also applicable to study of hybrid robots that are composed of different structures of parallel modules, where the number of links of the mechanisms is increased and the value of total degrees-of-freedom is augmented.

R E F E R E N C E S

[1] *Tsai, L-W.*, Robot analysis: the mechanics of serial and parallel manipulator, Wiley, 1999

[2] *Merlet, J-P.*, Parallel robots, Kluwer Academic, 2000

[3] *Di Gregorio, R*., *Parenti Castelli, V.,* Dynamics of a class of parallel wrists, ASME Journal of Mechanical Design, 126**,** 3, pp. 436-441, 2004

[4] *Clavel, R.*, Delta: a fast robot with parallel geometry, Proceedings of 18th International Symposium on Industrial Robots, Lausanne, pp. 91-100, 1988

[5] *Tsai, L-W., Stamper, R.,* A parallel manipulator with only translational degrees of freedom, ASME Design Engineering Technical Conferences, Irvine, CA, 1996

[6] *Hervé, J-M., Sparacino, F*., Star. A New Concept in Robotics, Proceedings of the Third International Workshop on Advances in Robot Kinematics, Ferrara, pp.176-183, 1992

[7] *Angeles, J.,* Fundamentals of Robotic Mechanical Systems: Theory, Methods and Algorithms, Springer, 2002

[8] *Wang, J., Gosselin, C*., A new approach for the dynamic analysis of parallel manipulators, Multibody System Dynamics, Springer, 2, 3, pp. 317-334, 1998

[9] *Tsai, L-W., S. Joshi, S*., Kinematics analysis of 3-DOF position mechanisms for use in hybrid kinematic machines, ASME Journal of Mechanical Design, 124, 2, pp. 245–253, 2002

[10] *Tanev, T.K.*, Kinematics of a hybrid (parallel–serial) robot manipulator", Mechanism and Machine Theory, Elsevier, 35, 9, pp. 1183-1196, 2000
[11] *Ibrahim, O., Khalil, W.*, Inverse and direct dynamic models of hybrid robots", Mechanism and Machine Theory, Elsevier, 45, 4, pp. 627-640, 2000
[12] *Shahinpoor, M.,* Kinematics of a parallel-serial (hybrid) manipulator, Journal of Robotic Systems, 9, 1, pp, 17-36, 1992,
[13] *Cheng, H.H., Lee, J.J., Penkar, R.*, Kinematic analysis of a hybrid serial-and-parallel-driven redundant industrial manipulator, International Journal of Robotics and Automation, 10, 4, pp. 159-166, 1995
[14] *Zhang, C., Song, S-M.,* Geometry and position analysis of a novel class of hybrid manipulators, Proceedings of ASME Design Technical Conference, Minneapolis, Minnesota, DE Volume 72, September 11-14, pp. 1-9, 1994
[15] *Gallardo, J., Lesso, R., Rico, J.M., Alici, G.,* The kinematics of modular spatial hyper-redundant manipulators formed from RPS type limbs, Robotics and Autonomous Systems, Elsevier, 59, 1, pp. 12-21, 2011
[16] *Staicu, S.*, Dynamics of the 6-6 Stewart parallel manipulator, Robotics and Computer-Integrated Manufacturing, Elsevier, 27, 1, pp. 212-220, 2011
[17] *Staicu, S.*, Matrix modeling of inverse dynamics of spatial and planar parallel robots, Multibody System Dynamics, Springer, 27, 2, pp. 239-265, 2012
[18] *Li, Y., Staicu, S.*, Inverse dynamics of a 3-PRC parallel kinematic machine, Nonlinear Dynamics, 67, 2, Springer, pp. 1031-1041, 2012